SECOND LAW BASED ANALYSIS OF FLUID FLOW IN THE REGENERATOR OF PULSE TUBE REFRIGERATORS

A. Jafarian, M. H. Saidi* and S. Kazemzadeh Hannani

Center of Excellence in Energy Conversion, School of Mechanical Engineering
Sharif University of Technology, P.O. Box 11115-9567, Tehran, Iran
a-jafarian@mehr.sharif.edu - saman@sharif.edu - hannani@sina.sharif.ac.ir

*Corresponding Author

Abstract   As a necessary component, regenerator plays an important role in the refrigeration performance of the pulse tube refrigerator. The objective of this research is to investigate the flow characteristics in a porous regenerator of the pulse tube refrigerators, subjected to oscillating flow. The hydrodynamic and thermal behavior of the regenerator is investigated by considering porous media approach. The conservation equations are transformed by implementing the volumetric average scheme. Harmonic approximation technique is employed to derive an analytical solution. To investigate the system performance, second law analysis is performed in order to calculate the second law efficiency. The effect of geometry and operating key parameters on the regenerator performance are investigated as well. The developed model is able to predict the oscillating flow characteristics in the regenerator.

Keywords Oscillatory Flow, Porous Media, Entropy Generation, Regenerator

چکیده   بازیاب حرارتی به عنوان یک جزء کلیدی در سرماسازهای لوله ضربانی، نقـشی اساسـی در عملکـرد برودتی این سیستم ها دارد. در این مقاله رفتار هیدرودینامیکی و گرمایی بازیاب حرارتی بـه عنـوان یـک مبـدل حرارتی کارآمد با ساختار محیط متخلخل مورد بررسی قرار می‌گیرد. معادلات بقا در ارتباط با محـیط متخلخـل با استفاده از روش میانگین گیری حجمی تبـدیل شـده و روش تخمـین هارمونیـک بـرای ارائـه حـل تحلیلـی معادلات، به کار گرفته می‌شود. به منظور ارزیابی کارایی بازیاب حرارتی آنـالیز قـانون دوم ترمودینامیـک انجـام شده و بازده قانون دوم ترمودینامیک محاسبه می‌گردد. همچنین تاثیر هندسه و پارامترهای عملکـردی بـر رفتـار بازیاب حرارتی مورد بررسی قرار خواهد گرفت. مدل ارائه شده در این مطالعه توانایی پیشگویی مشخصه هـای میدان جریان نوسانی در بازیاب حرارتی را دارا می‌باشد.

1. INTRODUCTION

The use of very low temperatures for some product's applications such as in computer hardware, space, military, medicine, and electrical systems, requires the achievement of high performance cryogenic coolers. Pulse tube refrigerator as a reliable cryogenic cooler, contains no moving parts at its cold head, thus having considerable system advantages over most other types of cryogenic refrigerators such as Stirling and Gifford-McMahon. Figure 1 shows a schematic view of a double inlet pulse tube refrigerator. Generally, regenerator as a compact heat exchanger is a stainless steel tube filled with screen disks, or metal fibers. One end of the

regenerator is at high temperature and the other end is at low temperature, around 300 k and 70 k, respectively. Gas flows into and out of the regenerator periodically having pressure fluctuations through out. Basic pulse tube refrigerator (BPTR) was first introduced by Gifford, et al [1] in 1964. A modified geometry introduced by Mikulin [2] in 1985 with an orifice and a reservoir (OPTR). With this modified system, temperature levels out near 20 k with a single stage and 4 k with a second one were achieved respectively. In 1990, Zhu [3] achieved a new constructional solution to increase the efficiency of the orifice pulse tube refrigerator through applying an extra bypass, namely double inlet pulse tube refrigerator. The improvement of
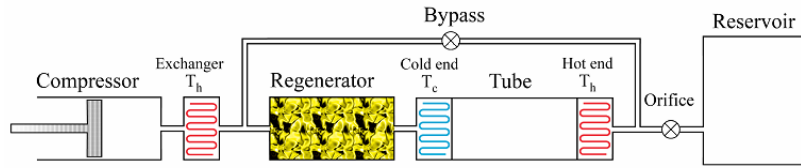
Figure 1. A schematic view of a double inlet pulse tube refrigerator.

the double inlet pulse tube refrigerator was achieved by implementing a bypass between the central zone of the Pulse tube and that of the thermal regenerator. This improvement led to a new configuration named, Multi Bypass Pulse Tube Refrigerator [4]. Further efforts have been made to improve the performance of the key components of the pulse tube refrigerator, as well as the complete cycle.

The significant influence of oscillating flow characteristics in the regenerator of pulse tube refrigerators, on cooling performance has recently been recognized in several works. These efforts are categorized into three subjects, namely types of the materials, experiments and modeling.

Waele, et al [5] investigated the energy and mass conservation equations of the regenerator in the case of steady state pulse tube with a linear expression for flow resistance of the material. Before that, Xiao, et al proposed a model, neglecting conduction effects. In addition, Swift, et al and Roach, et al, presented their theory based on thermo-acoustic effect and phasor analysis, respectively [5]. Kashani, et al [6] proposed an optimization program for modeling of the pulse tube cryocoolers. They proposed a perturbation solution for the regenerator. Gary, et al derived REGEN 3.2 model for regenerator analysis. REGEN is a finite difference program and is used to study the effects of regenerator geometry. Gedeon presented Sage Pulse Tube Model in 1999 [7]. Sage is one of the most comprehensive models for cryocooler analysis. This model provides the user the ability to model the cryocooler and perform optimization analysis as well. In 1999, Lewis, et al [8] considered the effect of regenerator geometry on pulse tube refrigerator performance. Further more, Harvey, et al [9] in 2003, proposed a comparative evaluation of numerical models for cryocooler regenerators.

In spite of numerous mentioned efforts which have been performed to analyze and optimize the performance of pulse tube refrigerators, little work has been done to consider the dissipative phenomena in the regenerator which is the main source of entropy generation and lost work. In addition, due to the complexity of the oscillatory compressible flow equations in porous media, proposed numerical and CFD models, usually take considerable time to perform system optimization. Our objective in the present study is to achieve a better understanding of the hydrodynamic and thermal phenomena occurring in the regenerator of Stirling type pulse tube refrigerators. In this respect, the entropy generation phenomena are investigated considering a complete system of compressible oscillating flow equations in the porous regenerator.

Harmonic approximation technique is employed to derive an analytical solution. To determine the optimum operating conditions that maximize the second law efficiency, entropy generation phenomena is considered. The proposed model provides the ability to analyze the flow characteristics of the regenerator and perform rapid optimization based on second law of thermodynamics.

2. PHYSICAL MODEL AND GOVERNING EQUATIONS

A double inlet Stirling type pulse tube refrigerator contains several components such as, a piston which generates pressure oscillations, a tube through which the working fluid flows freely, the stainless steel regenerator which acts as a compact heat exchanger, hot and cold heat exchangers which make proper thermodynamic contact with

the gas, an orifice, one bypass line and a reservoir. The regenerator geometry is a cylindrical domain with stainless steel wire screen mesh. Regenerator includes a solid and a fluid phase. The solid phase is assumed to be stainless steel packed wire screen with known thermal properties. The fluid phase is helium gas, which is assumed perfect. Figure 2 illustrates a schematic view of the regenerator.

The working process of the pulse tube refrigerator is complicated due to the nature of unsteady, oscillating compressible gas flow. To trace the process, we treat it as a one dimensional, periodic, unsteady compressible flow. Following assumptions are introduced in our model as well:

- The outer sidewall of the regenerator is thermally insulated.
- The gas is ideal, and the flow of the gas is laminar.
- The regenerator radius is much smaller than the regenerator length. Thus, the entrance effects are neglected.
- The fluid phase satisfies the no-slip condition on the fluid-solid interface.
- Porosity is constant.

Under the above mentioned assumptions, the mass, momentum and energy conservation equations and equation of state in the case of one-dimensional flow in the x-direction become:

$$\frac{\partial \rho_g}{\partial t} + \nabla \cdot (\rho_g \vec{u}) = 0 \tag{1}$$

$$\frac{\partial (\rho_g \vec{u})}{\partial t} + \nabla \cdot (\rho_g \vec{u}\, \vec{u}) = -\nabla P$$
$$+ \frac{1}{3} \nabla (\mu_g \nabla \cdot \vec{u}) + \nabla \cdot (\mu_g \nabla \vec{u}) \tag{2}$$

$$\frac{\partial (\rho_g e_g)}{\partial t} + \nabla \cdot (\rho_g \vec{u}\, En_g - k_g \nabla T_g) = 0 \tag{3}$$

$$(\rho C)_s \frac{\partial T_s}{\partial t} - \nabla \cdot (k_s \nabla T_s) = 0 \tag{4}$$

$$P = f(\rho_g, e_g) \tag{5}$$

$$T_g = f(\rho_g, e_g) \tag{6}$$

Table 1 represents the physical properties and operating data of a typical regenerator, for which the analytical solution has been carried out.

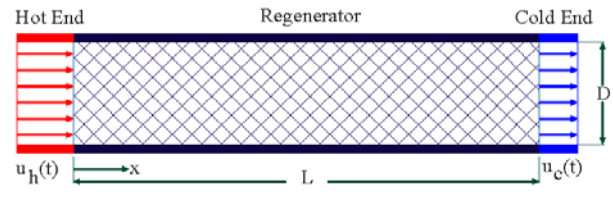The conservation equations for the solid matrix

Figure 2. A schematic view of the regenerator.

TABLE 1. Regenerator Physical and Operating Data.

Symbol	Unit	Value
$\overline{C}_p$	$(Jkg^{-1}k^{-1})$	5225
$\overline{C}_s$	$(jkg^{-1}k^{-1})$	368
d_{wire}	(mm)	5.6 E-2
D_h	(mm)	9.194 E-2
D	(m)	0.02
f	(Hz)	10
$\overline{k}_g$	$(Wm^{-1}k^{-1})$	0.1125
$\overline{k}_s$	$(Wm^{-1}k^{-1})$	12
K	(m^2)	3.40 E-11
L	(m)	0.2
P_m	(bar)	12
$\overline{T}_H$	(k)	300
$\overline{T}_C$	(k)	70
R_g	$(Jkg^{-1}k^{-1})$	2100
A_{pass}	(m2)	37 %
δ	(m)	0.001
$\overline{\mu}$	$(kgm^{-1}s^{-1})$	147.6 E-7
$\overline{\rho}_g$	(kgm^{-3})	3.8
ρ_s	(kgm^{-3})	8000
ε		0.6950

and gas phase are transformed by implementing the volume averaging technique. Volume averaging is an analytical method, used to unite the microscale and macroscale characteristic of porous media flows. Appling the volume averaging technique, the system of equations leads to:

$$\frac{\partial \rho_g}{\partial t} + \frac{\partial (\rho_g u)}{\partial t} = 0 \tag{7}$$

$$\frac{\partial (\rho_g u)}{\partial t} + \frac{\partial}{\partial x}(\rho_g u^2 + P) + \frac{\mu \varepsilon}{K} u + \rho_g u^2 \frac{\varepsilon^2 C_f}{\sqrt{K}} \frac{u}{|u|} = 0 \tag{8}$$

$$\frac{\partial (\rho_g e_g)}{\partial t} + \frac{\partial}{\partial x}(\rho_g u \, En_g - N_k k_g \frac{\partial T_g}{\partial x}) - h_{sg} A_s (T_s - T_g) = 0 \tag{9}$$

$$(\rho C_s) \frac{\partial T_s}{\partial t} - \frac{\partial}{\partial x}[k_s \tau_s \frac{\partial T_s}{\partial x}] + \frac{\varepsilon}{1-\varepsilon} h_{sg} A_s (T_s - T_g) = 0 \tag{10}$$

A variety of models can be considered to provide insight into the mechanism of net energy transport in the regenerator. Constant Temperature Model (CTM), Local Thermal Equilibrium Model (LTEM) and Dual Energy Equation Model (DEEM) are extensively used to analyze the energy transport in the porous media.

In the present study, Local Thermal Equilibrium Model (LTEM) has been employed as a moderate technique to achieve an analytical solution. This model assumes that the heat transfer between the gas and the matrix is perfect. The consequence of the assumption is that there is an infinitesimal temperature difference between the gas and matrix. LTEM results in a single energy equation with a single temperature for both solid and fluid phases.

Under the above assumption, the conservation equations and equation of state are now written as:

$$\frac{\partial \rho_g}{\partial t} + \frac{\partial (\rho_g u)}{\partial t} = 0 \tag{11}$$

$$\frac{\partial (\rho_g u)}{\partial t} + \frac{\partial}{\partial x}(\rho_g u^2 + P) + \frac{\mu \varepsilon}{K} u + \rho_g u^2 \frac{\varepsilon^2 C_f}{\sqrt{K}} \frac{u}{|u|} = 0 \tag{12}$$

$$[\rho_g C_v + (\rho C)_s \frac{1-\varepsilon}{\varepsilon}] \frac{\partial T}{\partial t} + \rho_g u C_v \frac{\partial T}{\partial x} + \frac{\partial}{\partial x}(Pu - N_k k_g \frac{\partial T}{\partial x} - \frac{1-\varepsilon}{\varepsilon} k_s \tau_s \frac{\partial T}{\partial x}) = 0 \tag{13}$$

$$P = \rho_g RT \tag{14}$$

Boundary conditions on the velocity and temperature are given as follows:

$$x = 0 \Rightarrow \begin{cases} u = \omega S_H \text{Real}(e^{i\omega t}) \\ k_r(1-\varepsilon)\frac{\partial T_r}{\partial x} = h_H(T_r - T_{HHX}) \end{cases} \tag{15}$$

$$x = L \Rightarrow \begin{cases} u = \omega S_C \text{Real}(e^{i(\omega t - \varphi)}) \\ k_r(1-\varepsilon)\frac{\partial T_r}{\partial x} = h_C(T_{CHX} - T_r) \end{cases} \tag{16}$$

In the above system of equations, the thermal coefficient of heat transfer at the cold head and hot end of the regenerator are calculated from the following correlation proposed by Nika [12] in the case of packed wire screens used in the Stirling engine:

$$Nu = \frac{hD_h}{k_g} = 0.33 Re_h^{0.67} \tag{17}$$

The permeability K, is expressed in terms of the pressure drop coefficient C_f and the Reynolds number based on hydraulic diameter, Re_h [12].

$$K = \frac{2\varepsilon D_h^2}{Re_h C_f} \tag{18}$$

Where:

$$Re_h = \frac{\dot{m} D_h}{\mu A_{pass}}$$

and

$$C_f = \frac{a}{Re_h{}^c} + b \qquad (19)$$

The value of the coefficients a, b and c for different situations can be found in [12,13]. In the present work, these coefficients were chosen from the empirical correlation found by Tanaka [13] for the oscillating flow.

3. SOLUTION PROCEDURE

Harmonic approximation technique is employed to derive an analytical solution. In this method, variables are expressed as a sum of mean value plus higher order terms. The terms of higher order than first-order are neglected in this technique. A product of two first order terms is assumed to be a second-order, while a product of a mean value and a first order term still remains first order. The values of the gas velocity, density, temperature and pressure can be written as:

$$u(x,t) = \text{Real}\,[\,u_1(x)e^{i\omega t}\,] \qquad (20)$$

$$\rho(x,t) = \rho_m + \text{Real}\,[\rho_1(x)e^{i\omega t}] \qquad (21)$$

$$T(x,t) = T_m + \text{Real}\,[T_1(x)e^{i\omega t}] \qquad (22)$$

$$P(x,t) = P_m + \text{Real}[P_1(x)e^{i\omega t}] \qquad (23)$$

Where, the real parts of the complex variables have been shown by the symbol Real. Substituting the above expressions into the system of equations and neglecting the second order terms, the following first order system of equations can be obtained:

$$\rho_1(i\omega) + \frac{\partial(\rho_m u_1)}{\partial x} = 0 \qquad (24)$$

$$\rho_m u_1(i\omega) + \frac{\partial P_1}{\partial x} + \frac{\mu\varepsilon}{K} u_1 = 0 \qquad (25)$$

$$[\rho_m C_u + (\rho C)_s \frac{1-\varepsilon}{\varepsilon}]T_1 e^{i\omega t} +$$

$$\rho_m u_1 C_u \frac{\partial T_m}{\partial x} e^{i\omega t} + \frac{\partial}{\partial x}(P_m u_1)e^{i\omega t} - \qquad (26)$$

$$(N_k k_g + \frac{1-\varepsilon}{\varepsilon} k_s \tau_s)(\frac{\partial^2 T_m}{\partial x^2} + \frac{\partial^2 T_1}{\partial x^2} e^{i\omega t}) = 0$$

$$\rho_1 = \frac{P_1}{R_g T_m} - \rho_m \frac{T_1}{T_m} \qquad (27)$$

Non-dimensional parameters are defined as:

$$x^* = \frac{x}{L}, \quad t^* = \omega t, \quad u^* = \frac{u}{u_0}, \quad P^* = \frac{P}{P_0}, \quad \rho^* = \frac{\rho}{\rho_0},$$

$$T^* = \frac{T}{T_H} \qquad (28)$$

Where, u_0, p_0 and ρ_0 represent the reference velocity, pressure and density respectively and are defined follows:

$$u_0 = \omega S_H, \quad \rho_0 = \frac{P_m}{RT_H}, \quad P_0 = \rho_0 \frac{u_0{}^2}{2} \qquad (29)$$

Expressing the equations versus non-dimensional parameters leads to:

$$\rho_1{}^* - i\beta_1 \frac{\partial(\rho_m{}^* u_1{}^*)}{\partial x^*} = 0 \qquad (30)$$

$$\rho_m{}^* u_1{}^* - i\beta_2 \frac{\partial P_1{}^*}{\partial x^*} - i\beta_3 u_1{}^* = 0 \qquad (31)$$

$$-i\beta_4 T_1{}^* e^{it^*} - \beta_5 \rho_m{}^* u_1{}^* \frac{\partial T_m{}^*}{\partial x^*} e^{it^*} -$$

$$\beta_6 \frac{\partial(P_m{}^* u_1{}^*)}{\partial x^*} e^{it^*} + (\frac{\partial^2 T_m{}^*}{\partial x^{*2}} + \frac{\partial^2 T_1{}^*}{\partial x^{*2}} e^{it^*}) = 0 \qquad (32)$$

$$\rho_1{}^* = \beta_7 \frac{P_1{}^*}{T_m{}^*} - \rho_m{}^* \frac{T_1{}^*}{T_m{}^*} \qquad (33)$$

Boundary conditions on the pressure and temperature are given as:

$$x^* = 0 \Rightarrow \begin{cases} u^* = \dfrac{1}{\beta_1} S_H^* \, Real(e^{it^*}) \\[2mm] \to \dfrac{\partial P_1^*}{\partial x^*} = -(\rho_m^* - i\beta_3) i \beta_8 S_H^* \\[2mm] \dfrac{\partial T_r^*}{\partial x^*} = \beta_9 (T_r^* - T_{HHX}^*) \end{cases} \quad (34)$$

$$x^* = 1 \Rightarrow \begin{cases} u^* = \dfrac{1}{\beta_1} S_C^* \, Real(e^{i(t^* - \varphi)}) \\[2mm] \to \dfrac{\partial P_1^*}{\partial x^*} = -(\rho_m^* - i\beta_3) i \beta_8 S_C^* e^{-i\varphi} \\[2mm] \dfrac{\partial T_r^*}{\partial x^*} = \beta_{10}(T_{CHX}^* - T_r^*) \end{cases} \quad (35)$$

Dimensionless parameters in the above equations have been defined in Table 2.

According to the results found in the literature [5,15] and the analysis performed in the present work, the magnitude of the second term in the right hand side of the Equation 33 is negligibly smaller than the first term. This means that the first order density is significantly a function of first order pressure rather than temperature. Thus, the second term can be neglected.

Since the outer surface of the regenerator wall is taken adiabatic, the cycle averaged net energy flow through the regenerator is independent of longitudinal position. The net energy flow in the regenerator includes the enthalpy flow by the gas, heat conduction through the regenerator solid phase, heat conduction through the gas and the regenerator wall. This rule can be used to calculate the mean temperature along the regenerator. The following statement represents the net energy flow along the regenerator of the cryocooler.

$$\dot{H} = [(\dot{m}C_p T_g) - k_s \tau_s (1 - A_{pass}) A_c \frac{\partial T_s}{\partial x} \\ - k_w A_{c,w} \frac{\partial T_w}{\partial x} - N_k k_g A_{pass} A_c \frac{\partial T_g}{\partial x}] \quad (36)$$

TABLE 2. Dimensionless Parameters in Equations.

Symbol	Definition
β_1	$\dfrac{u_0}{L\omega}$
β_2	$\dfrac{P_0}{\rho_0 u_0 L\omega}$
β_3	$\dfrac{\mu\varepsilon}{K\rho_0\omega}$
β_4	$\dfrac{\omega L \rho_0 [\rho_m C_v + (\rho C)_s \frac{1-\varepsilon}{\varepsilon}]}{(N_k k_g + \frac{1-\varepsilon}{\varepsilon} k_s \tau_s)}$
β_5	$\dfrac{\rho_0 u_0 C_v}{(N_k k_g + \frac{1-\varepsilon}{\varepsilon} k_s \tau_s)}$
β_6	$\dfrac{P_0 u_0}{T_H (N_k k_g + \frac{1-\varepsilon}{\varepsilon} k_s \tau_s)}$
β_7	$\dfrac{P_0}{\rho_0 R_g T_H}$
β_8	$\dfrac{\rho_0 L^2 \omega}{P_0}$
β_9	$\dfrac{h_H L}{k_s(1-\varepsilon)}$
β_{10}	$\dfrac{h_C L}{k_s(1-\varepsilon)}$
β_{11}	$\dfrac{P_0 u_0 L}{T_H N_k k_g}$

Here, we assumed the linear trend for the mean temperature along the regenerator to simplify the solution. Checking the cycle averaged net energy flow along the regenerator, it was observed that the linear profile satisfies the independency of net energy flow with respect to the longitudinal position precisely. Therefore a system of

differential equations in complex form is derived that should be solved to achieve the pressure gradient, density, velocity field and temperature distribution.

The steps which have been followed to achieve the solution are as:

- Substitute u_1^* and ρ_1^* from Equations 31 and 33 into the Equation 30 and solve the ordinary differential equation numerically to obtain the pressure amplitude, P_1^* as a function of longitudinal position, x.
- Put the first order pressure into Equation 31 to obtain the first order velocity, u_1^*.
- After substituting the first order velocity and the mean temperature distribution along the regenerator into Equation 32, solve the differential equation for the first order temperature numerically.
- Put the first order values obtained from solving the Equations 30-33 into the Equations 20-23 to complete the solution.

4. SECOND LAW ANALYSIS

One of the common criteria used to optimize the performance of the mechanical systems is the maximization of the 1st law efficiency. However, this parameter does not consider irreversibilities due to viscous and inertial effects, and heat flow. The second law efficiency can be defined by considering the rate of mechanical energy required to overcome the friction forces and all dissipative phenomena. The energy loss originated by the viscous dissipation and heat transfer are also included. The second law efficiency is defined by the following equation:

$$\eta_{2nd} = 1 - \frac{\langle \dot{W}_{loss} \rangle}{\langle \dot{W}_{tot} \rangle} \qquad (37)$$

Where, $\dot{W}_{tot}$ is the net work transfer rate to the gas to overcome the friction forces and dissipative phenomena. Symbol < > denotes integration over space and one period of time. The net work received by the working gas includes both acoustic

work and the work loss that should be compensated by the pressure generator in the system.

$$\langle \dot{W}_{ac} \rangle = \frac{1}{2\pi} \int_0^{2\pi} P \frac{dV}{dt} dt \qquad (38)$$

$$\langle \dot{W}_{loss} \rangle = \frac{1}{2\pi} \int_0^{2\pi} T_0 \dot{S}_{gen} dt \qquad (39)$$

The local entropy generation rate and lost work are given by:

$$\dot{S}_{g,gen} = \frac{N_k k_g}{T_g^2} (\frac{\partial T_g}{\partial x})^2 - \frac{u}{T_g} (\frac{\partial P}{\partial x}) \qquad (40)$$

$$\dot{S}_{s,gen} = \frac{k_s \tau_s}{T_s^2} (\frac{\partial T_s}{\partial x})^2 \qquad (41)$$

$$\dot{S}_{sys,gen} = \varepsilon \dot{S}_{g,gen} + (1-\varepsilon) \dot{S}_{s,gen} \qquad (42)$$

$$\dot{W}_{lost} = T_0 \int_0^L \dot{S}_{sys,gen} A_c dx \qquad (43)$$

Since the second law efficiency considers the total dissipation produced by irreversibilities in the system, it can be employed to optimize the operation of the regenerator section of the pulse tube cryocoolers by looking for values of the effective parameters that minimize entropy generation and so maximize the second law efficiency for suitable operating conditions.

Non-dimensionalized statements of the entropy generation are as follows:

$$\dot{S}^*_{g,gen} = \frac{1}{T_g^{*2}} (\frac{\partial T_g^*}{\partial x^*})^2 - \beta_{11} \frac{u^*}{T_g^*} (\frac{\partial P^*}{\partial x^*}) \qquad (44)$$

$$\dot{S}^*_{s,gen} = \frac{1}{T_s^{*2}} (\frac{\partial T_s^*}{\partial x^*})^2 \qquad (45)$$

$$\dot{S}^*_{sys,gen} = \varepsilon \dot{S}^*_{g,gen} + (1-\varepsilon) \dot{S}^*_{s,gen} \qquad (46)$$

Where, parameters $\dot{S}_{g,gen}$ and $\dot{S}_{s,gen}$ have been

non-dimensionalized by the statements $N_k k_g / L^2$

and $k_s \tau_s / L^2$, respectively.

5. RESULTS

To validate the proposed model, results have been compared with the experimental and numerical data in the literature. To perform the comparison between the results of the present model with that in the literature, two experimental and CFD works have been selected as target. The experimental work [14], deals with some experiments which have been conducted on the regenerator of a double inlet pulse tube refrigerator with operating pressure equal to 2.1 mPa, frequency of 16Hz and cold and hot temperatures of 77 k and 300 k, respectively. The CFD reference model is the Method of Line (MOL) solution, which has been applied to a typical regenerator with operating mean pressure of 3.1 mPa, frequency of 40 Hz and cold and hot temperatures of 70 k and 300 k, respectively [7]. Figures 3-6 show the results of the present work in comparison with those of the reference models. Figure 3 displays the temperature distribution along the regenerator. According to the above figure a good agreement between our solution and two reference works is observed.

Figure 4 monitors a small deviation between the outlet pressure profiles that is mainly due to the difference between the employed correlations of the inertia coefficient and permeability. Other vital parameters such as inlet and outlet density and velocity have been compared between the present solution and the CFD reference work, in Figures 5 and 6. In Figure 6 some deviations between the MOL solution and the present work are observed especially when the velocity is negative. These deviations are due to the effect of the last term in Equation 2, which has been neglected in our study as a second order term.

Figure 7 shows the velocity curves at different positions along the regenerator at frequency of 4Hz. According to the figure as the flow approaches the end of the regenerator, the velocity amplitude decreases. The effect of displacement length ratio, namely the ratio of the cold end
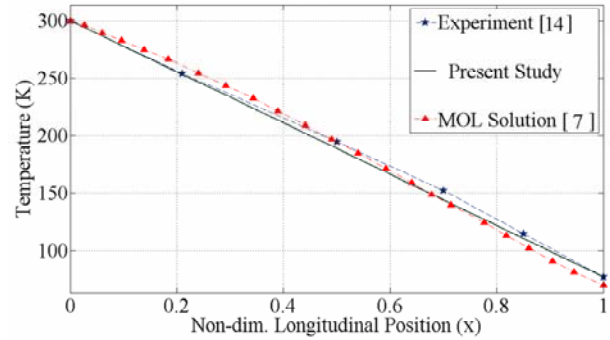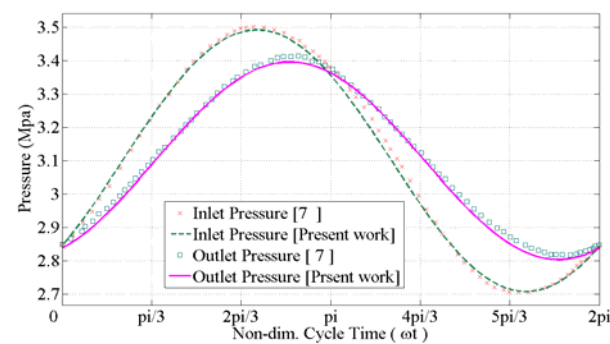

Figure 3. Regenerator temperature vs. position.

Figure 4. Inlet and outlet pressures vs. cycle time.
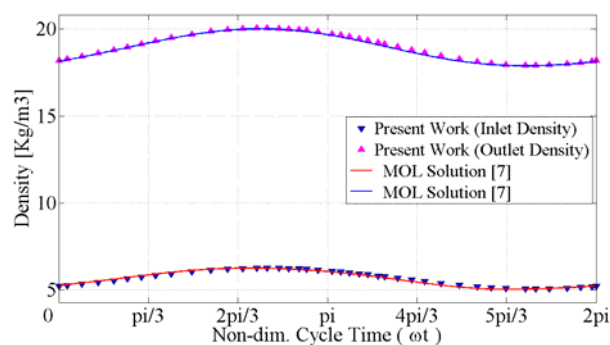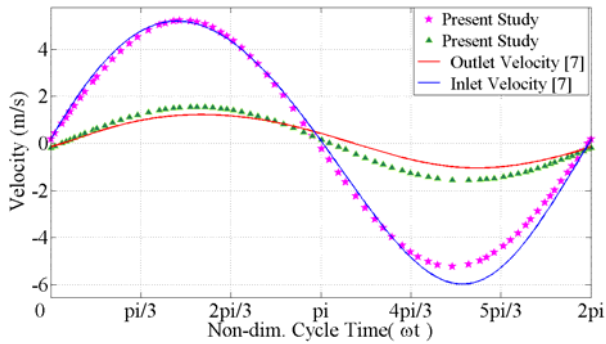

Figure 5. Helium density at the inlet and outlet of the regenerator vs. cycle time.

displacement length to the hot end on the velocity profile has been plotted in Figure 8. Here displacement length ratio, S_r is changed while keeping S_H constant and varying the S_c; where S_H and S_c represent the displacement length at the hot
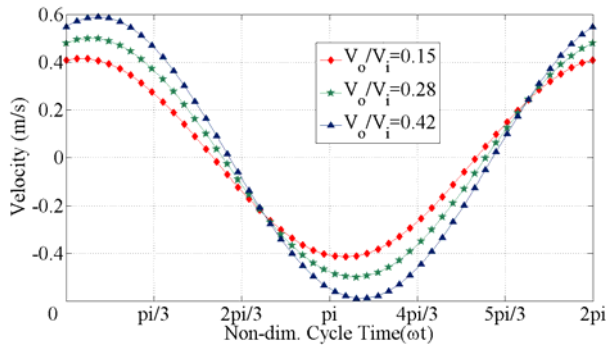
Figure 6. Regenerator inlet and outlet velocity vs. cycle time.
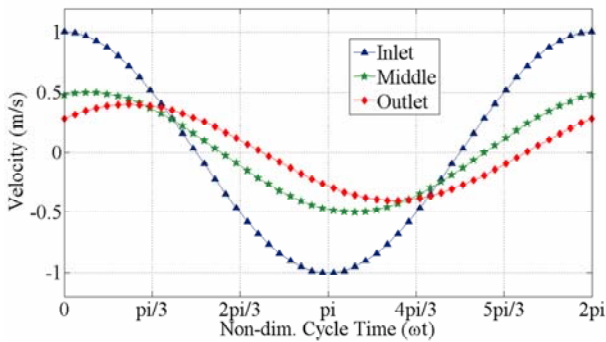
Figure 7. Velocity profiles in one period of oscillations at different locations along the regenerator.


Figure 8. Velocity profiles at the middle of the regenerator for different velocity ratios.

ratio of the outlet velocity to the inlet by changing the amount of displacement length ratio, S_r. Three velocity profiles have been plotted at the middle of the regenerator at frequency of 4Hz in Figure 8. We have varied S_r from 0.2 to o.6 to set the velocity ratio as displayed in the figure. Figure 9 displays the pressure distribution at different locations along the regenerator at frequency of 10 Hz. According to this figure, as the flow approaches the cold end of the regenerator, pressure amplitude decreases.

The influence of regenerator aspect ratio on the pressure amplitude along the regenerator has been shown in Figure 10. According to the above figure, pressure amplitude decreases as the flow goes toward the cold end. Changing the aspect ratio has been performed by varying the length and diameter, while keeping the regenerator volume constant. In addition, as Figure 10 displays the
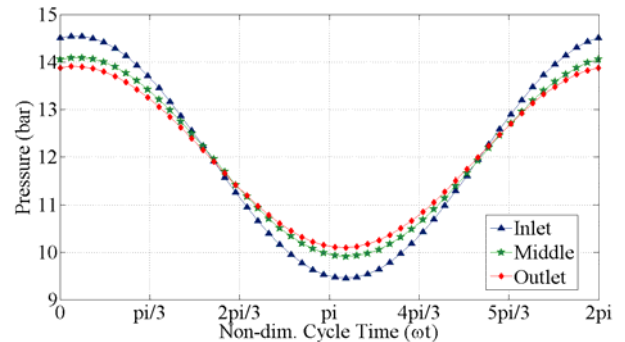
Figure 9. Pressure variation in one period of oscillations at different locations along the regenerator.

Figure 10. Pressure amplitude vs. position for several aspect ratios.
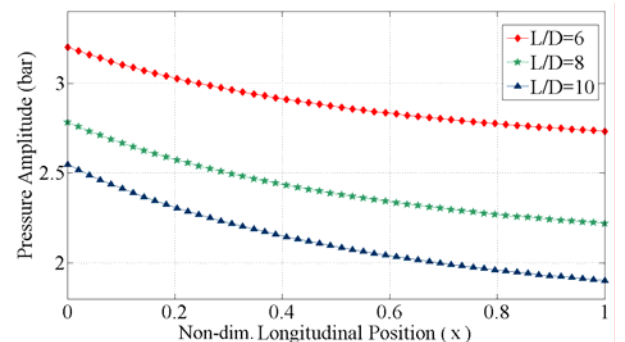
end and the cold end of the regenerator, respectively. In the orifice pulse tube refrigerator by closing the orifice valve, S_r approaches zero, otherwise $S_r < 1$. In the present work we set the

pressure amplitude decreases by increasing the amount of aspect ratio.

Figures 11 and 12 show the temporal variation of gas temperature for different values of the velocity inlet at frequency of 10 Hz. According to the figures, as the flow goes toward the cold end of the regenerator, temperature amplitude decreases. Besides, the temperature amplitude increases by increasing the amount of velocity inlet. In the regenerator, the temperature amplitude is very small in comparison with the average temperature. In fact, the large value of the solid matrix heat capacity results in very low amplitude.
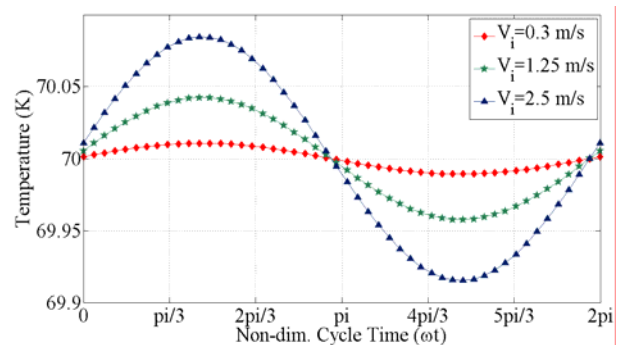
In Figure 13, the first order terms of the temperature, density and pressure have been plotted versus dimensionless cycle time in one period of oscillations. It is obvious that the amplitude of density is larger than the others. In addition, the amplitude of the first order temperature is negligibly smaller than the density and pressure amplitudes. This result approves the assumption that the first order density is more influenced by the pressure rather than temperature, used to simplify Equation 33.

Figures 14 and 15 show the entropy generation rate of the gas, matrix and sum of the two in one period of oscillations at the regenerator inlet and outlet at frequency of 6 Hz, phase shift angle equal to pi/4 and aspect ratio of 10. According to the above figures, the amplitude of total entropy generation decreases as the flow approaches the cold end of the regenerator. The total entropy in the regenerator is produced by conduction in the solid matrix, conduction in the working gas and inertia term. The amplitude of the produced entropy, by conduction effect in solid matrix and working gas is negligibly smaller than inertia effect. However, here due to the effect of inertia term that overcomes the conduction effect, the amplitude of total entropy generation decreases as the flow goes toward the cold end. In fact, the amplitude of entropy generation by the inertia effect at the cold end is significantly smaller than that of the hot end. It should be noted that the total entropy generation is the summation of the entropy generation in the solid and gas phases considering the porosity coefficient.

Figures 16-18 show the cycle averaged entropy generation versus position for several values of essential operating parameters of the regenerator.
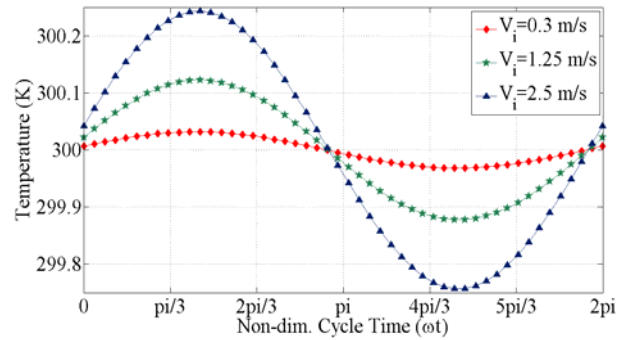
Figure 11. Temperature distribution at the hot end of the regenerator for different values of velocity inlet.
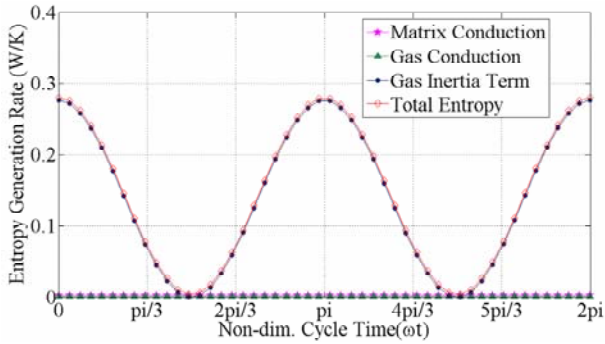

Figure 12. Temperature distribution at the cold end of the regenerator for different values of velocity inlet.
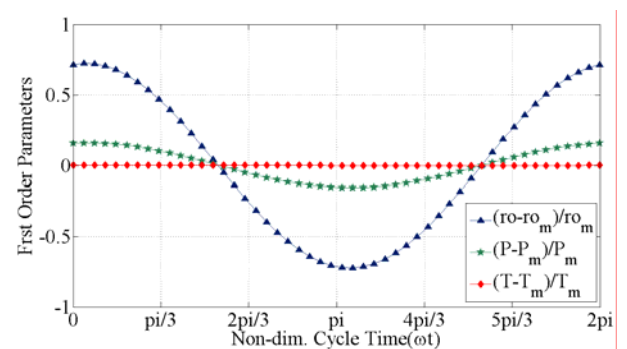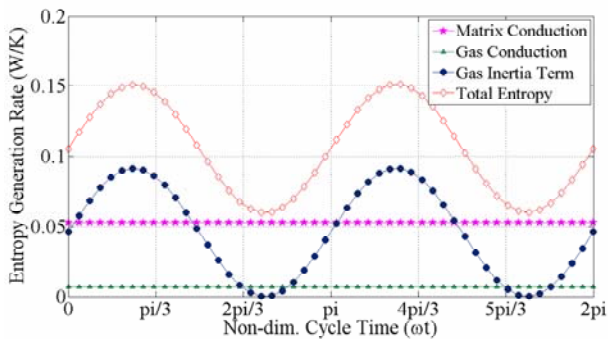

Figure 13. Comparison of the first order temperature, density and pressure.

In Figure 16, the influence of frequency has been displayed. According to the figure, increasing the frequency of oscillations leads to the increase of

Figure 14. Gas, matrix and total entropy generation rate in one period of oscillations at the regenerator inlet.
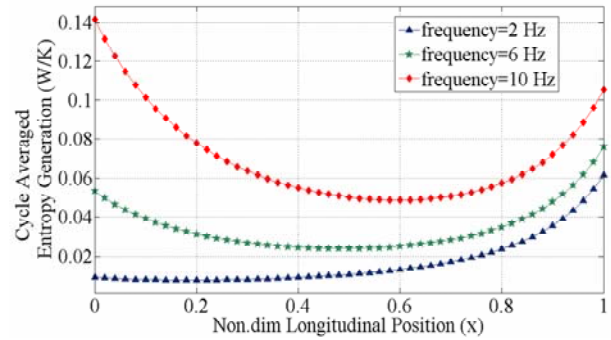

Figure 16. Total entropy generation vs. position at different frequencies.

Figure 15. Gas, matrix and total entropy generation rate in one period of oscillations at the regenerator outlet.

Figure 17. Total entropy generation vs. position at different phase shift angles.

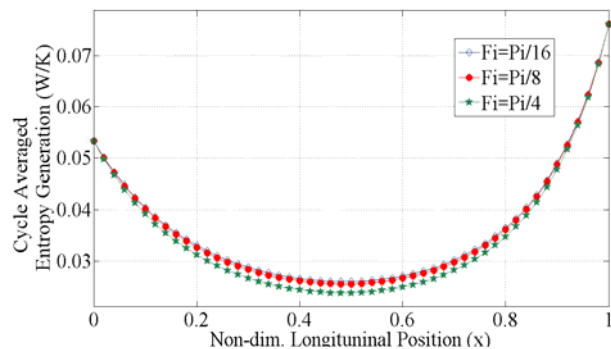**Figure 18**. Total entropy generation vs. position for different aspect ratios.

the cycle averaged entropy generation along the regenerator. In Figure 17, cycle averaged entropy generation has been plotted versus position for different velocity phase shift angles at f = 6 Hz. As it is shown in Figure 17, no significant variation is observed in the cycle averaged entropy generation along the regenerator by changing the phase shift angle. Figure 18 shows that while the aspect ratio is equal to 10, the entropy generation rate is minimum in comparison with other geometries. Smaller aspect ratio, results in more entropy generation as Figure 18 displays.

6. DISCUSSION

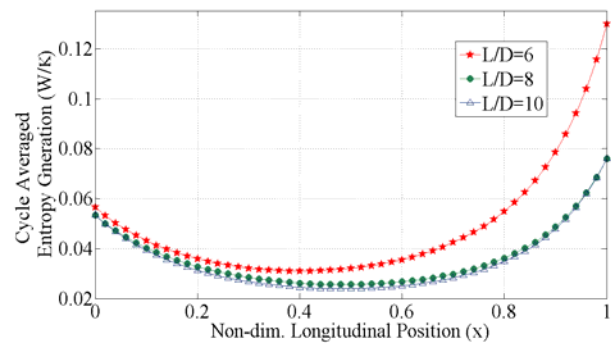Table 3 represents the summary result of the parametric study, which has been performed in the

present work. In this table, net work transferred to the gas, cycle averaged total entropy generation through the regenerator volume and the second law

efficiency has been displayed. According to the above table, as the frequency of oscillation increases, the cycle averaged entropy generation increases while an optimum occurs in the second law efficiency at frequency of 6 Hz.

By increasing the velocity phase shift angle, the second law efficiency increases significantly, as Table 3 shows. Phase shift angle in the regenerator is caused mainly by the pressure drop and the influence of orifice at the hot end of the tube section. Displacement length ratio has been employed in the present model to set the ratio of the outlet velocity to the inlet. Around 38 % increase occurs in the second law efficiency when the value of displacement length ratio increases from o.2 up to 0.6. The influence of the regenerator aspect ratio on the flow field second law efficiency has been considered in Table 3 as well. No significant variation is observed in the second law efficiency as the aspect ratio changes.

7. CONCLUSION

A one dimensional model for the regenerator of pulse tube refrigerators has been proposed in this research. The velocity and temperature fields for the oscillatory flow have been calculated analytically in order to apply the method of entropy generation minimization. To validate the model, results have been compared with the experimental and numerical data in the literature and a good agreement was observed. Further more, the behavior of several key parameters to reduce the entropy generation and hence increase the performance of the device was considered. Local thermal equilibrium model (LTEM) was employed in this study to simplify the analysis. The present model has the ability to be extended to, dual energy equation model with two separate equations for conservation of energy in the regenerator. The equations in the proposed model are generally

**TABLE 3. Net Work Transferred to the Gas, Cycle Averaged
Entropy Generation and Second Law Efficiency.**

Parameter	Value	Net Work Transfer Rate (W)	Cycle Averaged Entropy Generation (W/k)	2nd Law Efficiency (%)
f (Hz)	2	31.59	0.1024	53.45
	6	86.34	0.1973	59.81
	10	173.1	0.4349	51.04
φ	$\pi/16$	52.05	0.2075	29.6
	$\pi/8$	64.93	0.2054	44.19
	$\pi/4$	86.34	0.1973	59.81
S_r	0.2	56.55	0.1670	47.08
	0.4	86.34	0.1973	59.81
	0.6	117.6	0.2460	65.03
L/D	6	115.95	0.2789	60.59
	8	97.05	0.2250	60.4
	10	86.34	0.1973	59.81

valid and can be applied for different types of pulse tube refrigerators and especially for comparison of regenerator performance between various models such as orifice, double inlet, and multi bypass and multi stage systems.

8. NOMENCLATURE

$A(m^2)$	Area
$C(J/kg.k)$	Specific Heat Capacity
C_f	Inertia Coefficient
$D(m)$	Diameter
$e(J)$	Internal Energy
$En(J/kg)$	Gas Enthalpy
$h(W/m^2.k)$	Heat Transfer Coefficient
$\dot{H}(W)$	Net Energy Flow
$k(W/m.k)$	Thermal Conductivity
$K(m^2)$	Permeability
$L(m)$	Length
$\dot{m}(kg/s)$	Mass Flow Rate
N_k	Conductivity Enhancement
Nu	Nusselt Number
$P(bar)$	Pressure
$R(J/kg\ k)$	Gas Constant
Re	Reynolds Number
$Real$	Real Part
$r(m)$	Tube Radius
$\dot{S}(W/k)$	Entropy Generation Rate
$S(m)$	Displacement Length
$t(s)$	Time
$T(k)$	Temperature
$u(m/s)$	Velocity
$V(m^3)$	Volume
$\dot{W}(W)$	Rate of Work Transfer
$x(m)$	Axial Position

Subscripts

0	Reference State
1	First Order
ac	Acoustic
c	Cross Section
CHX	Cold Heat Exchanger
C	Cold End
g	Gas
gen	Generation
h	Hydraulic
H	Hot End
P	Constant Pressure
s	Solid
sg	Solid to Gas
HHX	Hot Heat Exchanger
m	Mean Value
max	Maximum
pass	Passage
r	Regenerator
s	Solid
sys	System
tot	Total
υ	Constant Volume
w	Wall

Superscripts

*	Non Dimensional
$-$	Average Value

Greeks

$\rho\ (kg/m^3)$	Density
$\omega\ (1/s)$	Angular Velocity
$\mu\ (kg/m.s)$	Dynamic Viscosity
$\nu\ (m^2/s)$	Kinematic Viscosity
$\delta\ (m)$	Wall Thickness
τ	Solid Tortousity
ε	Porosity
φ	Phase Shift Angle

9. REFERENCES

1. Popescu, G., Radcenco, V., Gragalian, E., Ramany and Bala, P., "A Critical Review of Pulse Tube Cryogenerator Research", *International Journal of Refrigeration*, Vol. 24, (2001), 230-237.
2. Mikulin, E. I., Tarasov, A. A. and Shkrebyonok, M. P., "Low Temperature Expansion Tubes", *Advances in. Cryogenic Engineering*, (1984), 629-637.
3. Zhu, S. W., Wu, P. Y. and Chen, Z. Q., "A Single Stage Double Inlet Refrigerator Capable of Reaching 42 k", *ICEC Proc. Cryogenics*, Vol. 13, (1990), 257-261.
4. Cai, J. H., Wang, J. J., Zhu, W. X. and Zhou, Y., "Experimental Analysis of Double Inlet Principle in Pulse Tube Refrigerator", *Cryogenics Journal*, (1993), 522-525.
5. De Waele, A. T. A. M., Hoojikaas, H. W. G., Steijaert, P. P. and Benshop, A. A. J., "Regenerator Dynamics in the Harmonic Approximation", *Cryogenics Journal*, Vol. 38, (1998), 995-1006.

6. Kashani, A. and Roach, P. R., "An Optimization Program for Modeling Pulse Tube Coolers", *Advances in Cryogenic Engineering*, Plenum Press, New York, U.S.A., Vol. 43, No. B, (1998), 1903-1909.

7. Harvey, J., "Oscillatory Compressible Flow and Heat Transfer in Porous Media-Application to Cryocooler Refrigerators", Ph.D. Thesis, Georgia Institute of Technology, Georgia, U.S.A., (2003), 113-119.

8. Lewis, M., Kuriyama, T., Xiao, J. and Radebaugh, R., "Effect of Regenerator Geometry on Pulse Tube Refrigerator Performance", *Advances in Cryogenic Engineering*, Plenum Press, New York, U.S.A., Vol. 43, (1998), 1999-2005.

9. Harvey, J., Desai, P. and Kirkconnell, C., "A Comparative Evaluation of Numerical Models for Cryocooler Regenerators", *Cryocoolers Journal*, Kluwer Academic, New York, U.S.A., Vol. 12, (2003), 547-554.

10. Neveu, P. and Babo, C., "A Simplified Model for Pulse Tube Refrigeration", *Cryogenics Journal*, Vol. 40, (2000), 191-201.

11. He, Y. L., Huang, J., Zhao, Ch. F. and Liu, Y. W., "First and Second Law Analysis of Pulse Tube Refrigerator", *Applied Thermal Engineering*, Vol. 26, (2006), 2301-2307.

12. Nika, Ph., Bailly, Y., Jeanot, J. C. and Labachelerie, M. D., "An Integrated Pulse Tube Refrigeration with Micro Exchangers: Design experiment", *International Journal of Thermal Science*, Vol. 42, (2003), 1029-1045.

13. Tanaka, M., Yamashita, I. and Chisaka, F., "Flow and Heat Transfer Characteristics of the Stirling Engine Regenerator in an Oscillating Flow", *JSME International Journal*, Vol. 33, (1990), 283-289.

14. Ju, Y. L., Wang, C. and Zhou, Y., "Numerical Simulation and Experimental Verification of the Oscillating Flow in Pulse Tube Refrigerator", *Cryogenics Journal*, Vol. 38, (1998), 169-176.

15. Beak, S. H., Jeong, E. S. and Jeong, S., "Two-dimensional Model for Tapered Pulse Tubes Part 1: Theoretical Modeling and Net Enthalpy Flow", *Cryogenics Journal*, Vol. 40, (2000), 379-385.